Heat transfer through homogeneous multilayered roofs in non air-conditioned rooms: experiments and simulations

J. Rojas[a], G. Barrios[a], G. Huelsz[a], R. Tovar[a], S. Jalife-Lozano[b]

[a] *Centro de Investigación en Energía, Universidad Nacional Autónoma de México Priv. Xochicalco s/n, Col. Centro, 62580 Temixco, Mor., Mexico*
[b] *Meccano de México, Antonio Dueñez 170, Zona Industrial, 27019, Torreón, Coah., Mexico*

Abstract

Heat transfer through the envelope walls and roofs is of fundamental importance for the thermal performance of a building. A time-dependent one-dimensional numerical model for the heat transfer through homogeneous multilayered walls and roofs in non air-conditioned rooms is presented. The model considers outdoor and indoor film heat transfer with constant coefficients, a given value of air changes per hour due to ventilation or infiltration, perfect and instantaneous mixing, and an adiabatic condition at a given distance from the wall or roof. Experimental data obtained from the roofs of two non air-conditioned full-scale test-huts, taken during a year in Torreón, Coahuila, Mexico, was used to validate the numerical model. The monthly average values of the outdoor surface temperature, of the indoor surface temperature, of the surface decrement factor, and of the surface lag time were used as parameters to compare numerical with experimental results. The agreement between these results validate the numerical model.

Keywords: heat transfer, roof, non air-conditioned, homogeneous layer

1. Introduction

The heat transfer through the envelope walls and roofs of a building is of fundamental importance for its thermal behavior. Most of the studies ad-

Email address: jrm@cie.unam.mx (J. Rojas)

dressing the time-dependent heat transfer through the envelope walls or roofs assume that the building is air-conditioned, *i.e*, the indoor air temperature is assumed to be held constant by a heating or cooling air-conditioned system.

Over the past 50 years, hundreds of building thermal performance software have been developed [1]. Most of the existing software employ the response factor analytical method (using or calculating conduction transfer function coefficients) and the finite volume or finite difference numerical methods for modeling the envelope walls and roofs [2]. Experimental studies to test analytical or numerical methods of the heat transfer through walls and roofs are scarce in the literature. They can be classified as laboratory simulation unit experiments [3, 4] and real situation experiments in full-scale test-huts [2, 5].

Ulgen [3] carried out laboratory experiments in a simulation unit considering a sinusoidal temperature change in the outdoor space and a non air-conditioned indoor space. He obtained analytical results from the solution of the one-dimensional heat transfer equation, under convective boundary conditions, using as input values the outdoor and indoor air temperatures. He compared the analytical and experimental results for ten wall configurations in terms of the surface decrement factor, DF_s, and surface lag time, LT_s, of the indoor surface temperature relative to the outdoor surface temperature. Maximum differences between experimental and analytical results were 0.31 for DF_s and 4.8 hours for LT_s.

Vijayalakshmi et al. [4] also carried out laboratory experiments in a simulation unit considering a sinusoidal temperature change in the outdoor space, but considering that the indoor space is air-conditioned. They reported numerical results of DF_s and LT_s obtained from the solution of the one-dimensional heat transfer equation for homogeneous multilayered walls with constant film coefficients, obtained with a finite differences method. They stated that the numerical values and the experimental ones differed by maximum of 18% for DF_s and by about 12% for LT_s. The differences were attributed to the non-uniformity in the material properties of the experimentally tested samples and the heat losses on the edges of the samples. When the effective thermophysical properties (i.e., the properties of the equivalent homogeneous layer, for example, considering the mortar in the brick wall) are used the differences decrease to 7% and 10%, respectively.

Kaşka et al. [5] made measurements in two air-conditioned test-huts over a period of 24 hours in the summer season of Gaziantep, Turkey. They measured inside and outside air temperatures, and surface temperatures of each

wall and roof layers for eight different walls and two different roofs. For each wall or roof, they analytically solved the one-dimensional heat transfer equation using a complex finite Fourier transform technique and they calculated the DF_s and the LT_s. Their theoretical and experimental results have a maximum difference of 0.06 for DF_s and 0.5 hours for LT_s.

Luo et. al. [2] measured surface temperatures and heat fluxes in walls of full-scale test-huts during a month. They did not specify whether the huts were or not air-conditioned. They studied five wall configurations. The surface temperatures were used to calculated the heat fluxes using analytical complex Fourier expansion, finite volume method, and conduction transfer function method, using two procedures to calculate the coefficients (that of Energy Plus software and the one proposed by the authors). In order to asses the performance of the different methods, they calculated heat fluxes and qualitatively compared the results to the experimental values. The authors conclude that all methods compared well with the measurements and discussed the small differences between methods found for the configurations studied.

The object of the present work is to validate a time-dependent one-dimensional numerical model for the heat transfer through homogeneous multilayered walls and roofs by comparing its results with experimental data obtained from the envelope roofs of non air-conditioned full-scale test-huts in a hot dry climate.

In Sec. 2, experiments in non air-conditioned test-huts are described. Sec. 3 presents the numerical model and Sec. 4 gives details of the numerical simulations. The comparison between experimental and numerical results is presented in Sec. 5. Conclusions are pointed out in Sec. 6.

2. Experiments

Experimental data was obtained during a year in two of the three one-room full-scale test-huts shown in Fig. 1, located in Torreón, Coahuila, Mexico, ($103^o24'$ west, $25^o30'$ north). The climate of this region is hot dry [6], with high mean solar radiation $18.3 MJ/m^2 day$ [7] and annual mean values of temperature 21.9^oC, amplitude of temperature oscillations 15.0^oC, and annual rainfall $232mm$ [8]. The test-huts had interior dimensions of $2.8m$ wide, $2.8m$ long and $2.7m$ high; their front walls were oriented 32.4^o west of geographic north. Each test-hut was built with different walls and roof configurations. Walls and roof of the test-hut 1 (in the middle of Fig. 1) were

Figure 1:
Test-huts in Torreón, Coahuila, Mexico.

made of a homogeneous $10cm$ thick aereated concrete monolayer; those of the test-hut 2 (on the right of Fig. 1) were made of two homogeneous layers, a $2cm$ thick thermal barrier layer at the outdoor side and a $8cm$ thick high-density concrete layer at the indoor side. The two roof configurations are presented, from exterior to interior layers, in Table 1. The roofs R1 and R2 correspond to each of the test-huts. The thermal properties of the materials are given in Table 2 [9]. Exterior walls and roofs were painted in white, having solar absorptance $A = 0.2$. The floor consisted of a $10cm$ thick reinforced concrete slab-on-ground. Each test-hut had a door on the left side of the front wall and a small window on top of the door. A circular window with a diameter of $20cm$ was located on the rear wall, with an internet-remote-controlled fan, S&P model HCM180, to propitiate forced ventilation. For the experiments reported here, both windows remained open and the fan was turned on for night ventilation from 21:15 to 8:00 hours, and windows were closed and fan turned off during the rest of the day.

For each test-hut, temperatures were measured at the central position of the exterior and interior surfaces of the roof with T-type AWG 30 thermocouples. The thermocouple junctions were stuck to the surfaces with high conductivity cement. For each test-hut a Davis Vantage Pro2 weather station was used to measure the indoor air temperature and humidity. The

Table 1:
Roof configurations. Description is given from exterior to interior layers and the layer thickness is in parentheses. Materials: aereated concrete (AC), thermal barrier (TB), and high-density concrete (HDC).

Code	Description
R1	AC (10cm)
R2	TB (2cm) + HDC (8cm)

Table 2:
Thermal properties of the different materials used in the configurations. Materials: aereated concrete (AC), thermal barrier (TB), and high-density concrete (HDC) [9].

Material	k W/m^oC	ρ kg/m^3	c J/kg^oC
AC	0.696	2180	940
TB	0.186	835	1987
HDC	0.816	2650	915

thermocouples and the weather station were connected to a Campbell Scientific data acquisition system, composed by a CR800 datalogger, an AM16/32 multiplexer and a RF401 radio. Both acquisition systems transmitted the data to another RF401 radio connected to a NL100 network link interface and to an internet modem.

The climatic conditions were registered using a Davis weather station, Vantage Pro2 plus, with rain collector, anemometer, temperature, pressure, humidity, UV, and solar radiation. The Vantage Pro2 Plus console had an acquisition data card and internet connection for data transmission.

All data was sampled every ten minutes during a year, from April 2010 to March 2011. The monthly average values of the ambient temperature, solar energy, and wind speed are presented in Table 3.

3. Model

The time-dependent one-dimensional numerical model for the heat transfer through homogeneous multilayered walls and roofs of N layers and total

Table 3:
Monthly average values of the ambient temperature, T_a, solar energy, E_s, wind speed, V_{met}, and outdoor film heat transfer coefficient h_{out} of Torreón, Coahuila, Mexico. Values are taken from April 2010 to March 2011.

Month	Data	T_a ^oC	E_s MJ/m^2day	V_{met} m/s	h_{out} $W/m^2\ ^oC$
1	01/2011	14.2	13.3	0.90	8.3
2	02/2011	16.4	16.4	1.34	9.5
3	03/2011	23.3	18.8	1.19	9.1
4	04/2010	23.5	24.2	2.14	11.8
5	05/2010	28.1	26.5	1.83	10.9
6	06/2010	29.0	26.0	1.97	11.3
7	07/2010	26.6	22.4	1.73	10.6
8	08/2010	28.9	25.2	1.63	10.4
9	09/2010	26.0	20.2	1.44	9.8
10	10/2010	23.0	20.0	0.90	8.3
11	11/2010	18.0	16.1	1.31	9.4
12	12/2010	14.4	13.5	0.57	7.3

thickness L (m), is based on the time-dependent one-dimensional heat transfer equation for the j-th layer [10],

$$\frac{\partial T}{\partial t} = \alpha_j \frac{\partial^2 T}{\partial x^2}, \tag{1}$$

where α_j (m^2/s) is the thermal diffusivity of the j-th material layer , T (^oC) the temperature, which is a function of the position inside the layer, x (m), and the time, t (s) .

In all unions between layers, the temperature is a continuous function and the heat transfer is equal at both sides [10], expressed as

$$k_j \left.\frac{\partial T}{\partial x}\right|_{(j,j+1)^-} = k_{j+1} \left.\frac{\partial T}{\partial x}\right|_{(j,j+1)^+}, \tag{2}$$

where k_j and k_{j+1} (W/m^oC) are the thermal conductivities of the j-th and $(j+1)$-th layers, respectively, and $(j, j+1)^-$ and $(j, j+1)^+$ denote that the derivative is evaluated left-hand and right-hand, respectively, in the interface of the j-th and $(j+1)$-th layers.

The outdoor boundary condition is considered a convection surface condition [10]

$$-k_1 \left.\frac{\partial T}{\partial x}\right|_{x=0} = h_{out}(T_{sa} - T(x=0)), \tag{3}$$

where h_{out} $(W/m^2\ ^oC)$ and $T(x=0)$ (^oC) are the film heat transfer coefficient and the temperature on the outdoor surface, respectively. The sol-air temperature T_{sa} (^oC) of the previous Eq. is defined by [11]

$$T_{sa} = T_a + I\frac{A}{h_{out}} - F, \tag{4}$$

where T_a (^oC) is the instantaneous temperature of the outdoor air, I (W/m^2) the instantaneous solar radiation, A $(-)$ the solar absorptance, and F (^oC) the infrared radiation factor [11]. The indoor boundary condition is also considered a convection surface condition [10]

$$-k_N \left.\frac{\partial T}{\partial x}\right|_{x=L} = h_{in}(T(x=L) - T_{in}), \tag{5}$$

where h_{in} $(W/m^2\ ^oC)$ and $T(x=L)$ (^oC) are the film heat transfer coefficient and temperature on the indoor surface, respectively, and T_{in} (^oC) is the indoor air temperature.

The model considers that T_{in} is a function of time and depends only on the heat transfer through the wall or roof under analysis and the ventilation or infiltration. Applying energy conservation [10]

$$d\rho_a c_a \left(\frac{dT_{in}}{dt}\right) = h_{in}(T(x=L) - T_{in}) + d\rho_a c_a C\frac{1h}{3600s}(T_a - T_{in}), \tag{6}$$

where ρ_a (kg/m^3) and c_a $(J/kg\ ^oC)$ are the density and specific heat of air and d (m) is the distance from the indoor side of the wall or roof to a place inside the room where an adiabatic or symmetry condition can be assumed, $(d \gg L)$, and C $(1/h)$ is the number of air changes per hour due to infiltration. This equation relates the temporal change in thermal energy of the air inside the room, where perfect and instantaneous mixing is assumed, and the heat transfer by convection between the air and the wall or roof indoor surface and by infiltration. This model could be extended to consider the heat transfer through walls, windows, ground, and ventilation, as in Refs. [12, 13], but for the purpose of having a model for wall or roof

configuration evaluation, this extension is not done in the present study. The model presented here is the same to the one used in Ref. [14] for a room with no air-conditioning, and is used in what follows to simulate the time-dependent heat transfer through two configurations of homogeneous multilayered roofs of non air-conditioned test-huts.

4. Numerical simulations

The heat transfer equations (1) and (6), with the corresponding boundary conditions, are solved employing an explicit finite volume scheme [15], programmed in C. The numerical simulations use experimental data of ambient temperature T_a and global radiation from one year of measurements, taken every ten minutes, as input data. Since the roofs are horizontal, the solar radiation on each, I, is the measured global radiation, $F = 3.9^oC$ [11], and $d = 2.5m$. The value of the indoor film heat transfer coefficient is taken as $h_{in} = 6.6W/m^{2o}C$ [16], the air changes per hour by infiltration from 8:00 to 21:15 hours is $C = 0.5\ 1/h$, and due to night ventilation from 21:15 to 8:00 hours is $C = 10.0\ 1/h$ [17]. The outdoor film heat transfer coefficient is calculated for each month using the model proposed by McAdams [18], which Palyvos [19] casts in SI units as $h_{out} = 5.7 + 3.8V_H$, where V_H is the monthly average wind speed at the roof height, $H = 2.7m$. The wind speed reported in Table 3 V_{met} was measured at a height of $H_{met} = 11m$, and both the meteorological station and the test-huts were in suburban areas, thus $V_H = V_{met}(H/H_{met})^{0.22}$ (see p. 16.3 of Ref. [11]). The monthly values of the outdoor film heat transfer coefficient h_{out} obtained by this procedure are reported in Table 3.

The numerical process is divided into two stages, a pre-warming and the simulation corresponding to the measurements period. For the pre-warming stage, a time-periodic T_a is constructed using the model proposed by Chow and Levermore [20]. This model requires the maximum and minimum values of T_a, the hour at which the maximum of T_a occurs, and the maximum value of I. These values are taken from the first day of measurements. The model also needs the hour at wich the minimum of T_a occurs, which is taken as the hour of sunrise. The initial condition for T and T_{in}, $T(x, 0)$ and $T_{in}(0)$, are taken as the mean value of T_a during the first day. The numerical simulation is iterated until it reaches a time-periodic condition. This condition is assumed to be obtained at time $t_r = 24n$ for which

$|T(x,t_r) - T(x,t_r+24)| < 0.1^oC$ for all x, T being in degrees Celsius, t_r in hours, and n an integer number.

The values of T and T_{in} obtained at the end of the pre-warming stage are used as initial values for the simulation of the measurements period stage. For this stage, T_a and I are taken from the measured data. The time step of the numerical simulation is smaller than the acquisition time-step, therefore a linear interpolation of the experimental data of T_a and I is used.

5. Results

For a qualitative comparison, the experimental and numerical indoor surface temperatures during a week in the hot season and during a week in the cold season for $R1$ and $R2$ roof configurations are presented in Figs. 2 and 3, respectively. For both roof configurations, the qualitative agreement between the experimental and numerical indoor surface temperatures can be observed during the two weeks. To examine the effect of air changes in the numerical indoor surface temperature, the results without any ventilation or infiltration, *i.e.* $C = 0$, are included. As can be observed the difference between numerical indoor surface temperature with night ventilation and diurnal infiltration and numerical results with $C = 0$ are small, this is due to the high thermal mass of both roof configurations.

A quantitative comparison between experimental and numerical results is made using, as parameters, the monthly average values of: the outdoor surface temperature $\overline{T_{es}}$, the indoor surface temperature $\overline{T_{is}}$, the surface decrement factor $\overline{DF_s}$, and the surface lag time $\overline{LT_s}$.

For each day, the surface decrement factor DF_s, and surface lag time LT_s are calculated, for both experimental and numerical results. The surface decrement factor is

$$DF_s = \frac{T_{is_{max}} - T_{is_{min}}}{T_{es_{max}} - T_{es_{min}}}, \tag{7}$$

where $T_{is_{max}}$ and $T_{is_{min}}$ are the maximum and minimum of the indoor surface temperature during a day, respectively, and $T_{es_{max}}$ and $T_{es_{min}}$ are the maximum and minimum of the outdoor surface temperature, respectively. The surface lag time is

$$LT_s = t(T_{is_{max}}) - t(T_{es_{max}}), \tag{8}$$

where $t(T_{is_{max}})$ and $t(T_{es_{max}})$ are the time of day when the indoor surface and outdoor surface temperatures reach their maximum values, respectively.

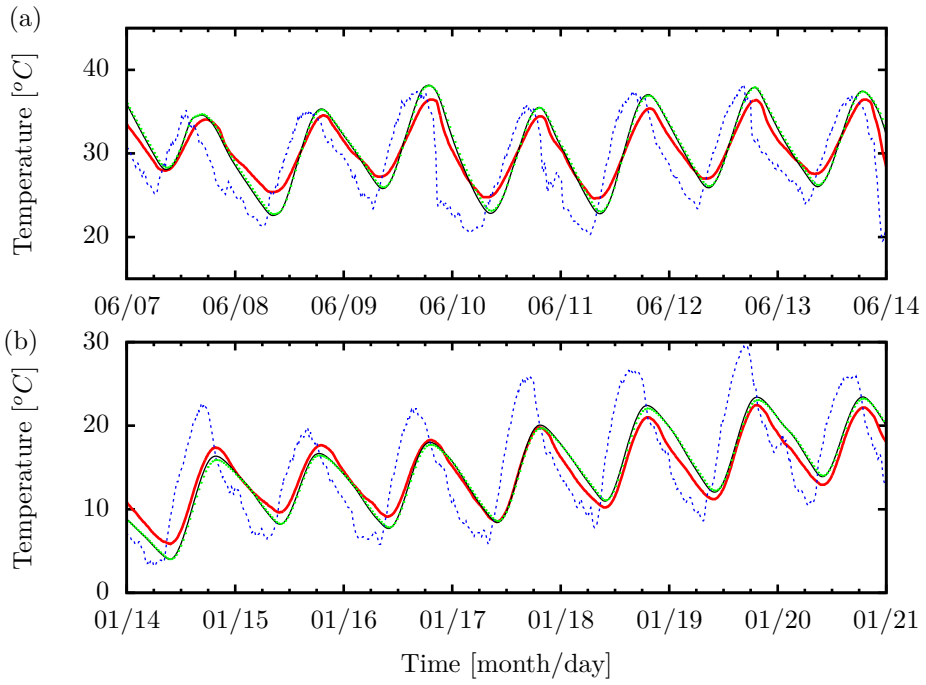

Figure 2: (Color online.) Experimental indoor surface temperature (red) continuous thick line, and numerical indoor surface temperature (black) continuous line, (a) during a week in the hot season and (b) during a week in the cold season, for $R1$. As a reference, the outdoor temperature (blue) dashed line is included. Also the numerical indoor surface temperature for $C = 0$ is included (green) dotted line.

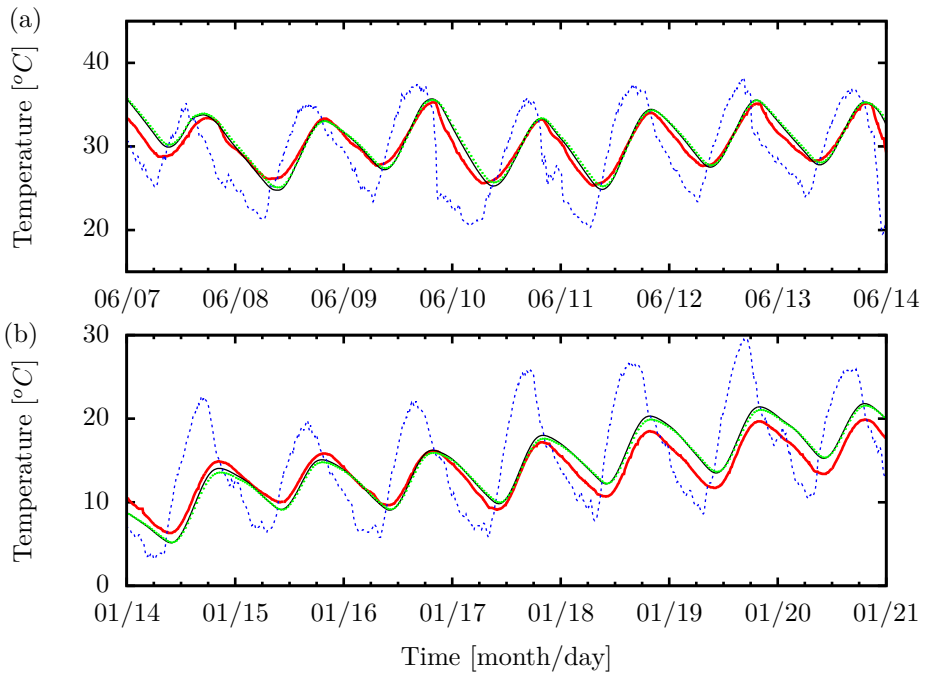

Figure 3: (Color online.) Experimental indoor surface temperature (red) continuous thick line, and numerical indoor surface temperature (black) continuous line, (a) during a week in the hot season and (b) during a week in the cold season, for $R2$. As a reference, the outdoor temperature (blue) dashed line is included. Also the numerical indoor surface temperature for $C = 0$ is included (green) dotted line.

In Figs. 4 and 5 experimental and numerical monthly average values of the outdoor surface temperature $\overline{T_{es}}$, of the indoor surface temperature $\overline{T_{is}}$, of the surface decrement factor $\overline{DF_s}$, and of the surface lag time $\overline{LT_s}$, for $R1$ and $R2$ roof configurations, are shown respectively. It can be observed that numerical values of $\overline{T_{es}}$, $\overline{T_{is}}$ and $\overline{DF_s}$ are in good agreement with experimental values for both roof configurations. The maximum difference for $\overline{T_{es}}$ is 2.6^oC (1.0^oC on average for both R1 and R2), for $\overline{T_{is}}$ it is 2.1^oC (average 0.8^oC), and for $\overline{DF_s}$ it is 0.07 (average 0.04). The numerical simulations overvalue $\overline{LT_s}$ with a maximum difference of 1.9 hours and an average of 1.6 hours. This difference may be due to the assumption of perfect and instantaneous mixing of the indoor air made in the numerical model. The number air changes has a small effect on the numerical values of these parameters. Comparing results for $C = 0$ relative to results for night ventilation and diurnal infiltration, the differences of $\overline{T_{is}}$ and $\overline{DF_s}$ have a maximum of 0.3^oC and 0.02 respectively.

The agreement between numerical and experimental results validate the one-dimensional numerical model for the heat transfer through homogeneous multilayered walls and roofs presented in Sec. 3. The maximum differences obtained in the present work for $\overline{DF_s}$ and $\overline{LT_s}$ are the same order of magnitude of those reported in Refs. [3] and [5].

6. Conclusions

Experimental data obtained from the envelope roofs of two non air-conditioned full-scale test-huts in real conditions, taken during a year in Torreón, Coahuila, Mexico, was used to validate the proposed time-dependent one-dimensional numerical model for the heat transfer through homogeneous multilayered walls and roofs in non air-conditioned rooms.

The model considers outdoor and indoor film heat transfer with constant coefficients, a given value of air changes per hour due to ventilation or infiltration, perfect and instantaneous mixing, and an adiabatic condition at a given distance from the wall or roof. The values of these parameters are given. Experimental ambient temperature and global radiation, taken every 10 minutes, were used as input data for the numerical simulations. For each month, the value of the outdoor film heat transfer coefficient was calculated using the wind speed monthly average.

The monthly average values of the outdoor surface temperature $\overline{T_{es}}$, of the indoor surface temperature $\overline{T_{is}}$, of the surface decrement factor $\overline{DF_s}$, and of the surface lag time $\overline{LT_s}$ were used as parameters to compare numerical with

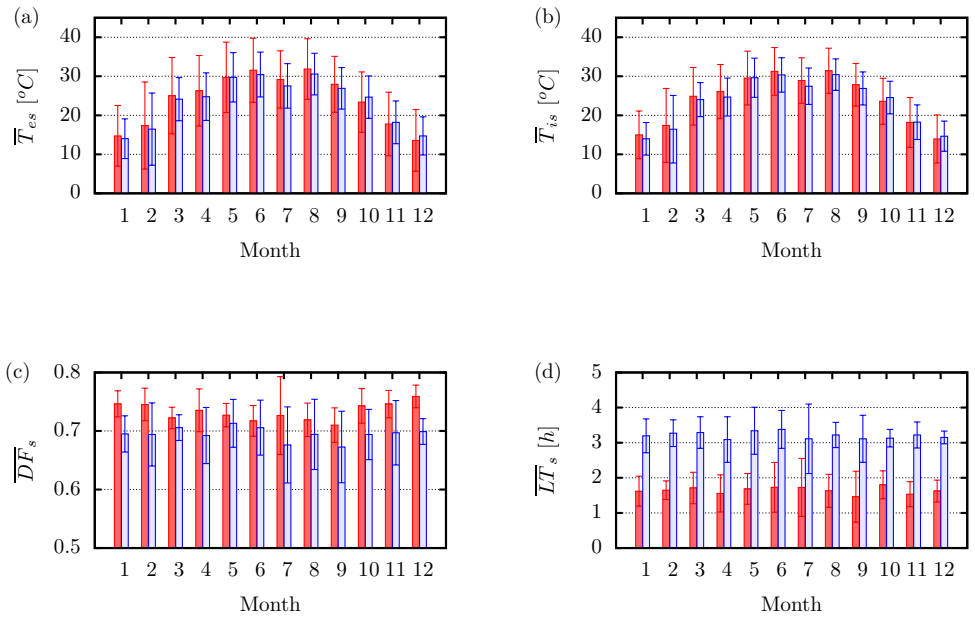

Figure 4: (Color online.) Experimental (red) dark gray, and numerical (blue) light gray, monthly average values of (a) the outdoor surface temperature $\overline{T_{es}}$, (b) of the indoor surface temperature $\overline{T_{is}}$, (c) of the surface decrement factor $\overline{DF_s}$, and (d) of the surface lag time $\overline{LT_s}$, for $R1$ roof configuration. The corresponding standard deviations are indicated.

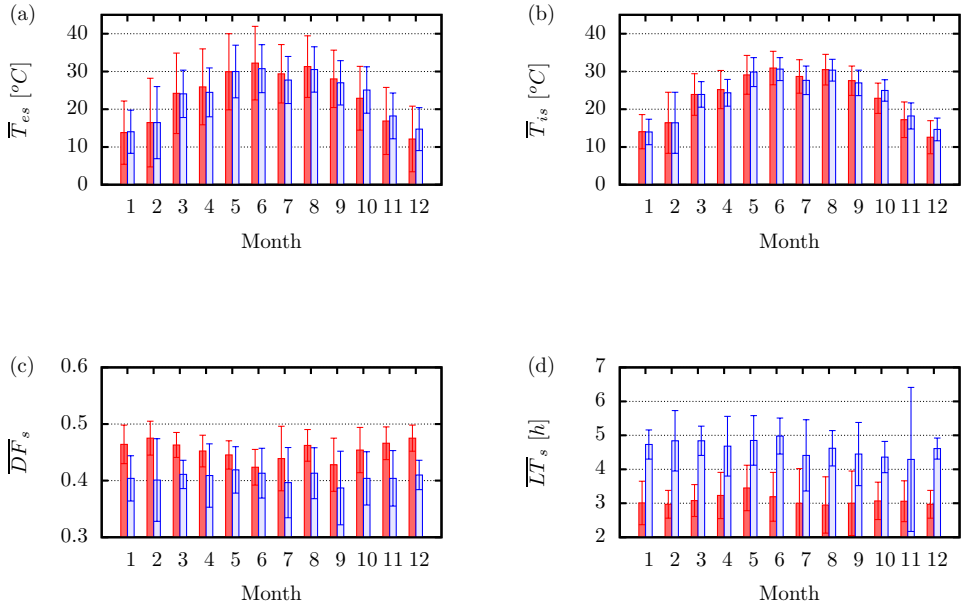

Figure 5: (Color online.) Experimental (red) dark gray, and numerical (blue) light gray, monthly average values of (a) the outdoor surface temperature $\overline{T_{es}}$, (b) of the indoor surface temperature $\overline{T_{is}}$, (c) of the surface decrement factor $\overline{DF_s}$, and (d) of the surface lag time $\overline{LT_s}$, for $R2$ roof configuration. The corresponding standard deviations are indicated.

experimental results. These results validate the one-dimensional numerical model for the heat transfer through homogeneous multilayered walls and roofs.

The effect of air changes in the numerical simulations was examined. The evaluated parameters obtained with and without ventilation or infiltration are very similar, this is due to fact that all these parameters are based on surface variables, and that both roof configurations have high thermal mass.

Acknowledgments

The authors thank Fabrisio Gómez and Guillermo Hernández for assistance in the experiments, and thank Héctor Cortés, Raúl Catalán, and Alejandro Onofre for assistance in data processing. Partial economic support from CONACYT 82109 and from Fondo CONACYT-Secretaria de Energía-Sustentabilidad Energética 118665 projects are acknowledged.

References

[1] D. B. Crawley, J. W. Hand, M. Kummert, B. T. Griffith, Contrasting the capabilities of building energy performance simulation programs, Building and Environment 43 (2008) 661–673.

[2] C. Luo, B. Moghtaderi, A. Page, Modelling of wall heat transfer using modified conduction transfer function, finite volume and complex fourier analysis methods, Energy and Buildings 42 (2010) 605–617.

[3] K. Ulgen, Experimental and theoretical investigation of effects of walls thermophysical properties on time lag and decrement factor, Energy and Buildings 34 (2002) 273–278.

[4] M. M. Vijayalakshmi, E. Natarajan, V. Shanmugasundaram, Thermal behaviour of building wall elements, Journal of Applied Sciences 6 (2006) 3128–3133.

[5] O. Kaşka, R. Yumrutaş, O. Arpa, Theoretical and experimental investigation of total equivalent temperature difference (tetd) values for building walls and flat roofs in turkey, Applied Energy 86 (2009) 737–747.

[6] Comisión Nacional de Vivienda, Código de Edificación de Vivienda, 2a Edición 2010. http://www.conavi.gob.mx/documentos/publicaciones/CEV%20PDF.pdf, September 18 2012.

[7] I. Galindo, G. Cifuentes, Irradiación solar global en la República Mexicana: valores horarios medios, Programa Universitario de Energía, UNAM, Ciudad de Mexico, Mexico, 1996.

[8] Servicio Meteorológico Nacional, Normales climatológicas 1971-2000, Estación Torreón, http://smn.cna.gob.mx/climatologia/normales/estacion/coah/NORMAL05040.TXT , September 12 2012.

[9] IIM-UNAM, Measurements made by the Materials Researchs Institut of Universidad Nacional Autónoma de México, 2009.

[10] F. Incropera, D. DeWitt, Fundamentals of heat and mass transfer, John Wiley, 2007.

[11] ASHRAE, Handbook Fundamentals, SI Edition, American Society of Heating, Refrigerating and Air-Conditioning Engineers, 2005.

[12] S. Kaushik, M. Sodha, P. Bansal, S. Bhardwaj, Solar thermal modelling of a non-airconditioned building: evaluation of overall heat flux, Energy Research 6 (1982) 143–160.

[13] V. S. Majali, B. N. Prasad, A. K. Bhat, Solar thermal modeling of non-air-conditioned multi-zone building: evaluation of heat fluxes and room air temperatures, International Journal of Green Energy 5 (2008) 405–412.

[14] G. Barrios, G. Huelsz, R. Rechtman, J. Rojas, Wall/roof thermal performance differences between air-contidionted an non air-conditioned rooms, Energy and Buildings 43 (2011) 219–223.

[15] S. V. Patankar, Numerical heat transfer and fluid flow, Taylor & Francis, 1980.

[16] SENER, Norma oficial mexicana NOM-029-ENER-2011 para eficiencia energética en edificaciones.- Envolvente de edificios para uso habitacional, Diario Oficial. 9 de agosto (2011) 44–89.

[17] Soler and Palau, HCM Extractores Helicoidales, http://www.soler-palau.com.mx/ima/products/pdf/332_09172010_HCM.pdf, September 26 2012.

[18] W. McAdams, Heat Transmission, third ed., McGraw-Hill Kogakusha, Tokyo, Japan, 1954.

[19] J. Palyvos, A survey of wind convection coefficient correlations for building envelope energy systems modeling., Applied Thermal Engineering 28 (2008) 801–808.

[20] D. H. C. Chow, G. J. Levermore, New algorithm for generating hourly temperature values using daily maximum, minimum and average values from climate model, Building Serv. Eng. Res. Technol. 28 (2007) 237–248.